Available online at www.sciencedirect.com
SCIENCE DIRECT
Catalysis Today 104 (2005) 225–230
CATALYSIS TODAY
www.elsevier.com/locate/cattod

Low-temperature H_2 and N_2 transport through thin $Pd_{66}Cu_{34}H_x$ layers

Xiulian Pan *, Mirjam Kilgus, Andreas Goldbach [1]

Fraunhofer Institut für Grenzflächen- und Bioverfahrenstechnik, Nobelstrasse 12, 70569 Stuttgart, Germany

Available online 9 April 2005

Abstract

The single gas H_2 and N_2 permeability of a 4 μm thick dense fcc-$Pd_{66}Cu_{34}$ layer has been studied between room temperature and 510 °C and at pressure differences up to 400 kPa. Above 50 °C the H_2 flux exhibits an Arrhenius-type temperature dependence with $J_{H_2} = (5.2 \pm 0.3)$ mol m^{-2} s^{-1} exp[(-21.3 ± 0.2) kJ mol^{-1}/(R·T)]. The hydrogen transport rate is controlled by the bulk diffusion although the pressure dependence of the H_2 flux deviates slightly from Sieverts' law. A sudden increase of the H_2 flux below 50 °C is attributed to embrittlement.

Keywords: PdCu alloy; Hydrogen transport; Activation energy; Phase diagram

1. Introduction

The palladium–hydrogen system has been subject of many investigations due to a wide spread interest in solid state hydrogen diffusion, in H_2 storage and separation, and in catalysis of hydrogenation/dehydrogenation reactions [1–4]. Lately, the transport of H_2 through dense Pd layers has attracted renewed interest because of the advances in fuel cell technologies and abundant visions of hydrogen based power generation. In particular, Pd membranes are reconsidered for high-capacity small-scale H_2 purification devices, which are essential for turning the output of on-board reformers into an adequate feed for current polymer-electrolyte membrane fuel cells (PEM-FC) in automotive vehicles and other non-stationary applications. For practical reasons it will be necessary to operate such a device in a wide pressure and temperature range including ambient conditions, and for economic reasons the noble metal layers have to be kept at a minimum thickness, i.e. on the order of 1 μm. Although a large amount of work has been aimed at the preparation of Pd layers in that size range, there is still very little known about the transport mechanism and the general behavior in H_2 of such thin metal layers between room temperature and 300 °C, where pure Pd layers routinely embrittle in H_2 due to a wide miscibility gap in the PdH_x phase diagram [1,5].

The H_2 transport across a metal layer is a complex process that involves a series of steps including H_2 adsorption and dissociation on the surface, dissolution and diffusion of atomic H within the metal lattice, H release from the lattice and recombination on the opposite surface, and eventual desorption of molecular H_2 into the gas phase on the low-pressure side. In bulk metals the H_2 transport is controlled by the diffusion through the lattice, and under steady state conditions and at very low H/metal atomic ratios $w \ll 1$, the H_2 flux J_{H_2} follows Sieverts' law [3,4]:

$$J_{H_2} = \left(\frac{D_k}{lK_s}\right) \cdot (P_{feed}^{0.5} - P_{perm}^{0.5}) \quad (1)$$

where D_k is the diffusion coefficient, l the thickness of the diffusion barrier, K_s a solubility constant (Sieverts' constant), and P_{feed} and P_{perm} are the feed and permeate side pressures, respectively. In thin metal layers the surface processes gain importance. A recent computational study showed that the desorption step is likely to affect the overall H_2 transport rate when the metal layer thickness falls below

* Corresponding author. Present address: Dalian Institute of Chemical Physics, Zhongshan Road 457, Dalian 116023, China.
Tel.: +86 411 8437 9190; fax: +86 411 4694 447.
E-mail addresses: panxl@dicp.ac.cn (X. Pan), goldbach@cnrs-orleans.fr (A. Goldbach).
[1] Co-corresponding author. Present address: Centre de Recherche sur la Matière Divisée, 1 bis rue de la Férollerie, 45071 Orléans cedex 2, France. Fax: +33 238 25 5376.

0920-5861/$ – see front matter © 2005 Elsevier B.V. All rights reserved.
doi:10.1016/j.cattod.2005.03.049

10 μm [6], which should be readily detected in the low-temperature behavior of the H_2 transport. However, there are few studies that probed systematically the H_2 permeation through thin Pd membranes between room temperature and 200 °C at practically relevant H concentrations [7].

The miscibility gap in the PdH_x system extends between $0.03 < x < 0.6$ at room temperature and it separates a dilute solid solution of hydrogen from a hydride phase [8], which both have face-centered cubic (fcc) structures [1,9]. The dissolution of hydrogen in Pd is an exothermic process and accordingly the hydrogen solubility at a constant pressure decreases with temperature. However, the terminal hydrogen solubility in the solution increases while the minimum hydrogen content of the hydride phase decreases with increasing temperature and pressure, so that the two phases eventually coalesce into a single supercritical phase around 300 °C and above 2.0 MPa pressure [4,5]. The gap can also be closed by alloying with various transition metals, e.g. phase segregation should be suppressed at room temperature in hydrogenated Pd alloys with sufficiently high Ag or Cu content [1,3,4].

PdCu alloys have attracted attention recently, because some have a body centered cubic (bcc) structure, which exhibits a smaller volume expansion upon loading with hydrogen [10] and a much higher hydrogen diffusivity below 300 °C than Pd or PdAg alloys [4,11]. Pd and Cu form a continuous series of disordered fcc solid solutions above 600 °C and below when the Pd content exceeds 60 at.%, whereas discrete compounds dominate in the Cu-rich part of the PdCu phase diagram below that temperature threshold [9]. Ordered bcc phases are found in the vicinity of 50 at.% Cu, and at Cu contents higher than 70 at.% two more structure types exist with Cu_3Au-related lattices [9]. The bcc regime is surrounded by a 2-phase region which extends up to 55 at.% Pd on the Cu-poor side, but accurate phase boundaries are not established below 400 °C. A hydrogen solution/hydride miscibility gap is known to form when alloys with less than 30 at.% Cu are exposed to H_2, however the critical alloy composition, temperature and pressure are not exactly known above which this gap disappears [12–14]. The H_2 permeation of PdCu layers of varying composition has been studied in the temperature range between 200 and 600 °C [15,16], but little is known about the permeation properties and phase stability of PdCu alloys in thin layers at lower temperatures [16], although this will be crucial for the long term operation of such membranes in practical devices.

In this contribution we present a study of the H_2 and N_2 permeation through a 4 μm thick $Pd_{66}Cu_{34}$ layer between room temperature and 510 °C. This alloy has an fcc structure, and it borders to the hydrogen solution/hydride miscibility gap that exists in the Cu-poor section of the Pd–Cu–H system. On the other side the fcc/bcc 2-phase region begins at slightly larger Cu concentrations [9]. Thus it is within the narrow range, where fcc-PdCu alloys presumably do not undergo a phase transition between room temperature and 600 °C when kept in H_2. In the following we investigate the N_2 permeation through the hydrogenated metal layer, the rate controlling step of H_2 transport in this thin layer, and the impact of the low-temperature phase boundaries on the H_2 transport in this system.

2. Experimental

The preparation of Pd-seeded γ-Al_2O_3/α-Al_2O_3 capillaries and their sealing with ceramic glaze was previously described [17,18]. The α-Al_2O_3 support had an average pore size of 500 nm, a porosity of 50%, an outer diameter of 0.8 mm and a 0.2 mm thick wall (Fig. 1(a)). It was furnished on the outer surface with a 5 μm thick γ-Al_2O_3 layer with 4–6 nm wide pores and 50% porosity and a 4 μm thick PdCu layer (Fig. 1(b)). Pd and Cu were successively deposited by electroless plating from a $PdCl_2$ bath [19] and a $Cu(NO_3)_2$ bath, the latter of which was adapted from Uemiya et al. [15] (Table 1). The alloy composition was initially controlled by weight and the deposition rate of each metal. The two metal layers were alloyed through annealing in N_2 at 500 °C for 12 h. Prior to the here described experiments the alloy layer

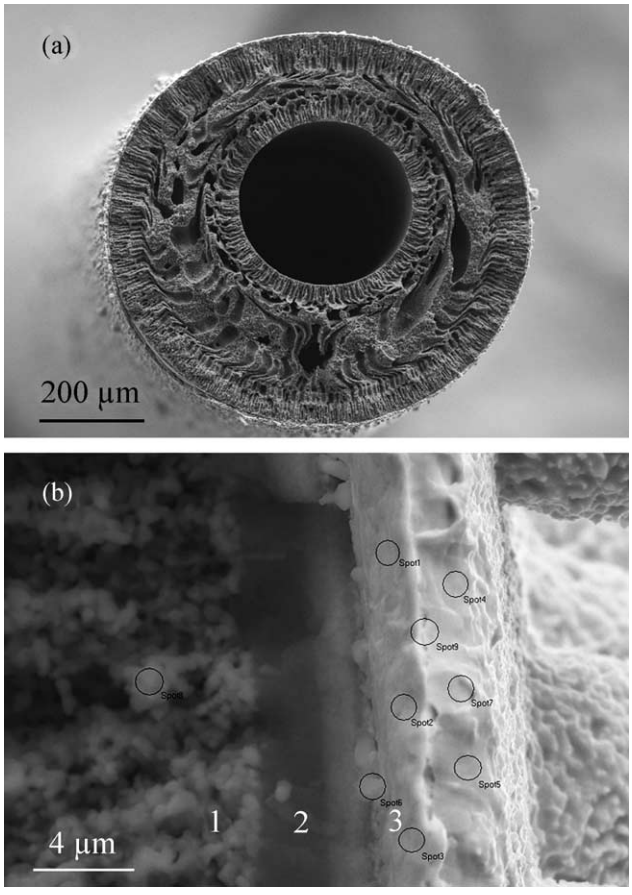

Fig. 1. SEM pictures of the PdCu/α-Al_2O_3 capillary membrane, which consists of layer 1: the α-Al_2O_3 support, layer 2: an intermediate γ-Al_2O_3 layer seeded with Pd nuclei, and layer 3: the PdCu layer on the outside.

Table 1
The compositions of Pd and Cu plating baths and the plating conditions

Plating process	Component	Quantity
Pd (T = 45 °C, pH 11)	$PdCl_2$	4.43 g l^{-1}
	$Na_2EDTA{\cdot}2H_2O$	37.22 g l^{-1}
	NH_3	134 g l^{-1}
	$N_2H_4{\cdot}H_2O$ (1 M)	17.5 g l^{-1}
Cu (T = 60 °C, pH 12)	$Cu(NO_3)_2{\cdot}2.5H_2O$	9.6 g/l
	$Na_2EDTA{\cdot}2H_2O$	29.8 g l^{-1}
	2,2-Bipyridyl	20 mg l^{-1}
	$K_4[Fe(CN)_6]{\cdot}3H_2O$	50 mg l^{-1}
	NaOH	11 g l^{-1}
	HCHO (≥36.5 wt.%)	125 ml l^{-1}

was further annealed at 530 °C in H_2 for 1 week [20] till the stabilization of the H_2 flux. EDX analyses yielded 66 ± 5 at.% Pd and 34 ± 5 at.% Cu and XRD confirmed the fcc structure.

A fiber was mounted with silicone glue into a test module for dead-end permeation experiments. The separation area was 2.7 cm^2 and the permeate side was kept at atmospheric pressure (P_{perm} = 98.5 kPa) with H_2 or N_2 (99.999% each) being fed on the shell side while the silicone seal was kept outside the furnace. After stabilization of temperature and pressure (24 h minimum) single gas fluxes J_{H_2} and J_{N_2} were measured with soap bubblemeters at room temperature (25 °C) and atmospheric pressure.

3. Results

Fig. 2 shows the temperature dependence of the H_2 flux between room temperature and 510 °C through the $Pd_{66}Cu_{34}$ layer at a trans-membrane pressure gradient $\Delta P_{H_2} = (P_{feed} - P_{perm}) = 350$ kPa. The maximum H_2 flux was $J_{H_2} = 0.19\ mol\ m^{-2}\ s^{-1}$ at 510 °C. Above 50 °C it is well represented by an Arrhenius-type function with J_{H_2}=(5.2 ± 0.3) mol m^{-2} s^{-1} exp[(− 21.3 ± 0.2) kJ mol^{-1}/($R{\cdot}T$)]. Below that the H_2 flux increased abruptly as the temperature decreased, which hints at a diminished integrity of the layer. Fig. 2 also shows the N_2 fluxes across the $Pd_{66}Cu_{34}$ and the $Pd_{66}Cu_{34}H_x$ layers. The latter rapidly formed when the metallic layer was exposed to H_2. Prior to H_2 exposure, the N_2 flux was $J_{N_2} = 4.2 \times 10^{-5}\ mol\ m^{-2}\ s^{-1}$ at room temperature and $J_{N_2} = 2.8 \times 10^{-5}\ mol\ m^{-2}\ s^{-1}$ at 510 °C and ΔP_{N_2} = 100 kPa.

We assessed the N_2 flux through the $Pd_{66}Cu_{34}H_x$ layer by monitoring the permeate flux after switching from H_2 to N_2 at the feed side. Fig. 3 shows the corresponding permeate fluxes at 200 and 510 °C, which pass through minima and then swing back to the N_2 flux levels measured before H_2 exposure. The $Pd_{66}Cu_{34}H_x$ does not instantaneously transform back into metallic $Pd_{66}Cu_{34}$ because the interstitial H has to diffuse to a surface and recombine before it is released to the gas phase. In the employed dead-end configuration this hydride-to-metal transformation is retarded because H_2 released on the feed side is trapped there. Thus it has to pass through the $Pd_{66}Cu_{34}H_x$ layer again to reach the low-pressure side where it is purged from the system. The permeate flux displayed in Fig. 3 consists of three components: H_2 diffusing through the metal lattice, H_2 passing through defects in the $Pd_{66}Cu_{34}H_x$ or the $Pd_{66}Cu_{34}$ layer, and N_2 permeating through those defects. The intake of H leads to an expansion of the metal lattice [1,21]. Consequently microscopic pinholes in the layer become smaller and the gas transport through them drops off in the

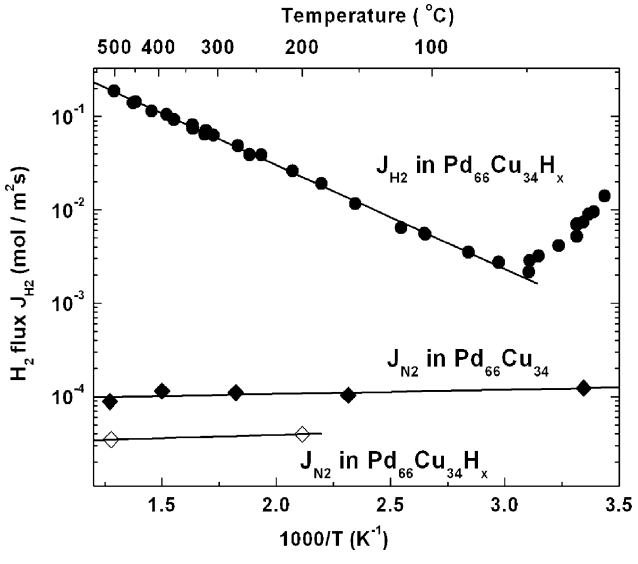

Fig. 2. Temperature dependence of the H_2 flux across the $Pd_{66}Cu_{34}H_x$ layer at ΔP_{H_2} = 350 kPa. Also included are N_2 fluxes through the $Pd_{66}Cu_{34}$ and $Pd_{66}Cu_{34}H_x$ layers (both J_{N2} are referred to ΔP_{N_2} = 350 kPa). Measurement errors are smaller than the data points.

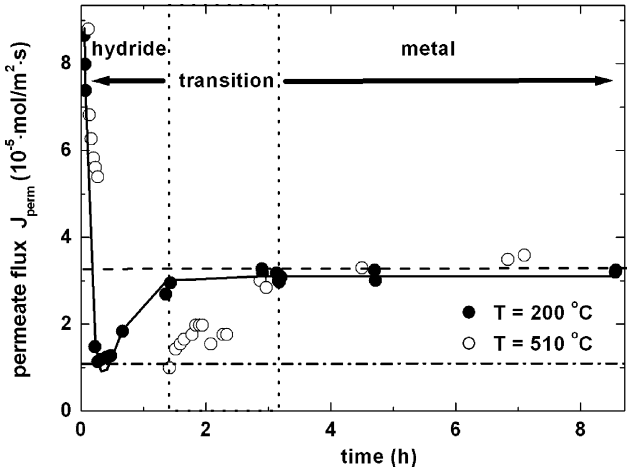

Fig. 3. Permeate fluxes through the $Pd_{66}Cu_{34}$ layer at 200 and 510 °C after switching from H_2 to N_2 on the feed side (ΔP_{N_2} = 100 kPa). The time scale of the 200 °C measurement is divided by 10 and the solid line is a guide to the eye of the corresponding permeate flux. The dashed line marks the N_2 flux level of the pristine metal layer in that temperature range. The dash-dotted line indicates the minimum permeate flux level. The zone between the dotted lines defines the hydride-to-metal transition during the measurement at 510 °C.

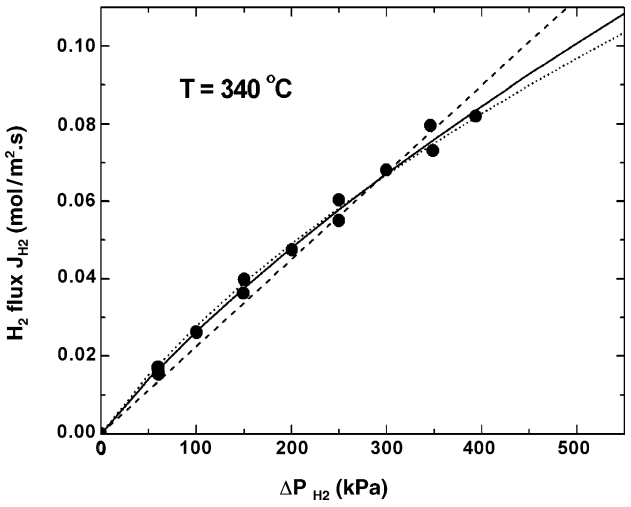

Fig. 4. Pressure dependence of the H_2 flux across the $Pd_{66}Cu_{34}H_x$ layer at 340 °C and $\Delta P_{H_2} = 350$ kPa. A Sieverts' type power law with a pressure exponent $n = 0.63$ yields the best fit (solid line). Curves corresponding to $n = 0.5$ (dotted) and $n = 1$ (dashed) have been included for comparison.

$Pd_{66}Cu_{34}H_x$ phase as can be seen in Fig. 3. When all hydrogen is released from the metal layer the pinholes open up again and the N_2 flux comes back to the level initially found for the hydrogen-free $Pd_{66}Cu_{34}$ layer. We identify this minimum flux $J_{N_2,min} = 1.1 \times 10^{-5}$ mol m^{-2} s^{-1} at $\Delta P_{N_2} = 100$ kPa as an upper limit for gas transport through defects in the $Pd_{66}Cu_{34}H_x$ layer.

We found that the N_2 flux increases linearly with pressure over the whole temperature range. Fig. 4 shows the pressure dependence of the H_2 flux at 340 °C. The experimental data can be fitted to the following equation:

$$J = A[(P_{feed})^n - (P_{perm})^n] \quad (2)$$

where $A = (D_k/lK_s)$. A least square fit yields a pressure exponent $n = 0.63 \pm 0.07$ and $A = (2.5 \pm 1.2) \times 10^{-3}$ mol m^{-2} s^{-1} kPa$^{-0.63}$. The pressure exponent is slightly larger than 0.5, which would be expected if bulk diffusion were the rate-limiting step and the H content of the alloy were within the infinite dilution limit (Sieverts' law). A rise of the pressure exponents towards 1 is expected when surface processes on the feed side gain importance (H_2 dissociative adsorption). This can occur when the solid-state diffusion time is sufficiently shortened at smaller metal layer thicknesses (Eq. (1)) and/or when the transfer of H from the gas phase into the metal lattice is slowed down at low feed side pressures. Thus, bulk diffusion should control the overall transport rate in thick layers and at high pressures, while surface processes could dominate the transport kinetics in sufficiently thin layers and at low pressures [22]. Fit curves pertaining to these high- and low-pressure limits ($n = 0.5$ and 1, respectively) are included in Fig. 4 for comparison. The quality of the fit corresponding to Sieverts' law is similar to that of the optimum fit yielding a prefactor $A = 6.7 \times 10^{-3}$ mol m^{-2} s^{-1} kPa$^{-0.5}$, but we note that the H/metal atomic ratio could be as high as 0.2 at the highest pressures applied in this study according to Flangan et al. [14] and thus could be outside the range where Sieverts' law strictly applies.

4. Discussion

The ratio between single gas H_2 and N_2 fluxes is frequently used to characterize the separation behavior of metal barriers, because dense layers are impervious to inert gases. This flux ratio is referred to as ideal hydrogen-to-nitrogen selectivity α_{H_2/N_2}. Here we obtain $\alpha_{H_2/N_2} \approx 2000$ at 510 °C and $\Delta P_{H_2} = 350$ kPa, which indicates that there are very few defects in this layer. However, this number is an underestimation by definition. The H_2 flux is generally compared to the N_2 flux through the metal layer prior to hydrogen exposure, i.e. the H_2 permeation of a metal hydride layer is correlated to the N_2 permeation of a neat metal layer. As can be seen from Fig. 3 the defect flux is significantly smaller through a nearly perfect metal layer when it is loaded with hydrogen. Based on the minimum defect flux one obtains a higher ideal selectivity of $\alpha_{H_2/N_2} \approx 5000$. One can also qualitatively assess the size of defects from the disparity between the defect fluxes through the $Pd_{66}Cu_{34}$ and the $Pd_{66}Cu_{34}H_x$ layers. The metal lattice expands a few percent upon the intake of hydrogen, e.g. in case of $Pd_{71}Cu_{29}$ the lattice constant a_0 increases from 3.823 to 3.873 Å when 0.2 H per metal atom are incorporated [13]. In order to have the observed impact on the N_2 permeation the effective defect size in the $Pd_{66}Cu_{34}$ layer has to be of the same order of magnitude as the kinetic diameter of N_2 (3.6 Å) [23], and thus it must be in the range of 1 nm. Larger pinholes will not shrink significantly when H is inserted into the metal lattice and the effect of the hydride-to-metal transformation on the N_2 flux should be less evident then.

Deviation of the pressure dependence from Sieverts' law is often interpreted as a sign of surface processes impacting the H_2 transport rate. However, the increased pressure exponent of 0.63 cannot be taken as such evidence considering that practically the same value was found in a recent study of the hydrogen permeability of 1 mm thick Pd sheets at pressures up to 2.76 MPa [24]. There is little doubt that bulk diffusion will control the hydrogen permeation rate in a Pd layer as thick as that. A more reliable approach to assess the rate-determining process of hydrogen permeation is its examination as a function of temperature. Usually diffusion and surface reactions differ significantly in their activation energies and a crossover between limiting steps in the transport should be detectable in the temperature dependence of the permeation rates. Fig. 2 shows a discontinuity around 50 °C, but above that the H_2 flux is well represented by a single Arrhenius-type function. This attests to a single process controlling the H_2 permeation above that temperature.

The hydrogen solubility and diffusivity will determine the temperature dependence if the H_2 transport is controlled

by bulk diffusion (Eq. (1)). The thermal dependence of the diffusion coefficient D_k can be expressed as follows [4,6]:

$$D_k = D_0 \exp\left(\frac{-E_D}{RT}\right) \quad (3)$$

D_0 is a frequency factor and E_D the activation energy for the diffusion. At infinite dilution, i.e. the H/metal atomic ratio $w \ll 1$, the solubility constant K_s in Eq. (1) can be written as [4,6]:

$$K_s = \exp\left[\left(\frac{\Delta\bar{H}^0_H}{RT} - \frac{\Delta\bar{S}^0_H}{R}\right)\right] \quad (4)$$

where $\Delta\bar{H}^0_H$ and $\Delta\bar{S}^0_H$ are the relative partial molar enthalpy and entropy of dissolution, respectively. The temperature dependence of the hydrogen flux across a metal barrier can be derived by combining Eqs. (1), (3) and (4) then:

$$J_{H_2} = J_0(P^{0.5}_{feed} - P^{0.5}_{perm}) \exp\left(\frac{-E_{perm}}{RT}\right) \quad (5)$$

where $J_0 = (D_0/l)\exp(\Delta\bar{S}^0_H/R)$ and $E_{perm} = E_D + \Delta\bar{H}^0_H$.

Partial molar enthalpies and entropies of hydrogen dissolution in fcc-PdCu alloys with up to 40 at.% Cu were determined by several groups [13,14,21,25]. Fisher et al. carried out the most comprehensive study and reported $\Delta\bar{H}^0_H = -8.3$ and -7.7 kJ mol^{-1} for alloys with 29 and 40 at.% Cu, respectively [13]. Thus we estimate $\Delta\bar{H}^0_H = -8$ kJ mol^{-1} for the molar enthalpy of hydrogen dissolution in $Pd_{66}Cu_{34}$. Activation energies are available for the diffusion of different hydrogen isotopes in selected fcc-PdCu alloys [11,26–28]. From a graphical presentation of hydrogen diffusion coefficients in $Pd_{47}Cu_{53}$ given by Völkl and Alefeld [11], a value can be derived very similar to the E_D = 33 kJ mol^{-1} obtained by Zetkin et al. for deuterium diffusion in the same alloy [26]. On the other hand, hydrogen diffusion in fcc-Pd is characterized by an activation energy of 22 kJ mol^{-1} [3], which we assume to be the minimum barrier in fcc-PdCu alloys. Hence, we estimate $22 < E_D < 33$ kJ mol^{-1} for hydrogen diffusion in $Pd_{66}Cu_{34}$, and from Eq. (5) we obtain a net activation energy $14 < E_{perm} < 25$ kJ mol^{-1} for hydrogen permeation through $Pd_{66}Cu_{34}$. This range compares well with E_{perm} = 21.3 kJ mol^{-1} resulting from the Arrhenius plot in Fig. 2. We conclude that the temperature dependence of the hydrogen permeation through the 4 μm layer can be satisfactorily explained by a bulk diffusion limited transport, and surface processes do not impact the hydrogen transport through the thin $Pd_{66}Cu_{34}$ layer even as room temperature is approached.

The rapid increase of the permeate flux by an order of magnitude between 50 and 20 °C indicates that embrittlement of the layer sets in. This could result from segregation of a hydrogen solution and a hydride phase. An early study suggested that the 2-phase region in the ternary Pd–Cu–H system could extend to slightly higher than 30 at.% Cu [13] and the opening of a miscibility gap could therefore account for the permeate flux increase below 50 °C. Yet, there is a second scenario, which merits consideration. Note, that the

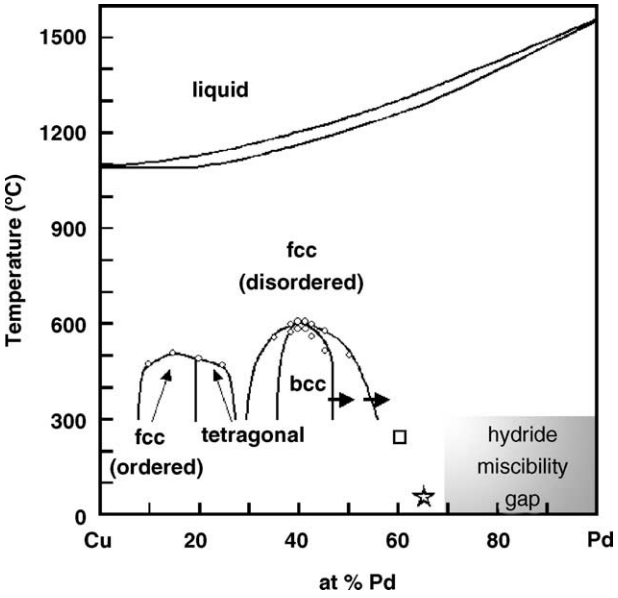

Fig. 5. PdCu phase diagram as obtained by Taylor [29], Jones and Sykes [30] (after Hansen [9]). In addition the hydride miscibility gap in Pd-rich alloys is indicated. The arrows mark the H_2-related phase boundary shift observed by Piper [31] and the square denotes a H_2-induced phase transition observed by Degtyareva et al. [32]. The star marks the discontinuity in the H_2 permeation found in this study.

EDX analysis of a second composite membrane, which had been plated together with the here studied one, yielded a metal layer composition of $Pd_{61}Cu_{39}$. This composition is very close to the fcc/bcc 2-phase region in the binary PdCu system. The commonly accepted PdCu phase diagram is based on the work of Taylor [29], Jones and Sykes [30], who studied PdCu alloys at temperatures above 400 °C. They placed the boundary of the fcc/bcc 2-phase region around 55 at.% Pd on the Cu-poor side (Fig. 5). However, Jones and Sykes also found that an alloy with 55 at.% Pd still contained 20 % ordered bcc-PdCu after cooling from 500 °C (fcc single phase) to 250 °C over a period of 4 months. Thus, the low-temperature phase boundaries are not well established in this system, and there is evidence that they shift under the influence of H_2. Piper observed that the fcc/bcc boundaries shift up to 3 at.% to lower Cu contents after annealing PdCu foils under 500 kPa H_2 pressure at 350 °C [31]. In addition, Degtyareva et al. reported an irreversible phase transition in fcc-$Pd_{60}Cu_{40}$ around 220 °C under H_2 pressures of 0.5–2 MPa, which was accompanied by a tetragonal distortion of the metal sublattice [32]. We have added those data and the discontinuity in the H_2 permeation found in this study to the phase diagram in Fig. 5, which also indicates the miscibility gap in the Pd–Cu–H system. It appears that the equilibrated fcc/bcc 2-phase region could extend up to ca. 65 at.% Pd on the Cu-poor side. Thus it cannot be excluded that the abrupt increase of the permeate flux below 50 °C is linked to coexisting incommensurate fcc and bcc hydride phases. Such a discontinuity must be clearly distinguished from the hydrogen solution/hydride miscibility gap, which exists at

lower Cu concentrations, because there both the solution and the hydride are based on fcc alloy phases. However, we have not observed a bcc phase in the posterior XRD characterization of the $Pd_{66}Cu_{34}$ layer. Although the bcc fraction could be below the detection limit, the opening of a hydrogen solution/hydride miscibility gap remains the better rationale for the break down of the $Pd_{66}Cu_{34}$ layer near room temperature. Nevertheless, this study provides evidence that low-temperature phase changes are likely in thin PdCu layers when kept in H_2, and that both the binary Pd–Cu and the ternary Pd–Cu–H phase diagram need to be reexamined.

5. Conclusion

The N_2 permeation indicated a good integrity of a 4 μm thick fcc-$Pd_{66}Cu_{34}$ layer, which was supported on an asymmetric alumina capillary membrane, yielding $J_{N_2} = 2.8 \times 10^{-5}\,\mathrm{mol\,m^{-2}\,s^{-1}}$ at 510 °C and $\Delta P_{N_2} = 100\,\mathrm{kPa}$. The N_2 permeation through the hydrogenated $Pd_{66}Cu_{34}H_x$ was considerably smaller under the same conditions, i.e. $J_{N_2} = 1.1 \times 10^{-5}\,\mathrm{mol\,m^{-2}\,s^{-1}}$, indicating that the size of pinholes was in the range of the kinetic diameter of the N_2 molecule. The temperature and pressure dependence of the H_2 permeation indicates that bulk diffusion is the rate determining process in the hydrogen transport between 50 and 510 °C and at pressure differences up to 400 kPa. At 510 °C and $\Delta P_{H_2} = 350\,\mathrm{kPa}$ the hydrogen flux was $J_{H_2} = 0.19\,\mathrm{mol\,m^{-2}\,s^{-1}}$ and the ideal H_2/N_2 selectivity was $\alpha(H_2/N_2) \approx 5000$. The obtained activation energy $E_{perm} = 21.3\,\mathrm{kJ\,mol^{-1}}$ is in good agreement with relative partial molar enthalpies for hydrogen dissolution and energy barriers for hydrogen diffusion in PdCu alloys.

Below 50 °C the $Pd_{66}Cu_{34}H_x$ layer deteriorated as evidenced by a rapid increase of the permeate flux. We presume that the hydrogen solution/hydride miscibility gap known for fcc phases in the ternary Pd–Cu–H system extends beyond the accepted upper limit of 30 at.% Cu. However, we note also that the low-temperature phase boundaries in this system are not very well established, and the formation of two incommensurable fcc and bcc PdCu hydride phases cannot be ruled out either. The knowledge of the phase behavior of thin Pd alloy layers down to ambient temperatures is essential for the advancement of related membrane technologies and detailed low-temperature structural investigations on these materials are highly desirable.

Acknowledgements

We thank Nicole Dinges for fabricating the ceramic capillaries and Monika Riedl for SEM measurements. Xiulian Pan acknowledges support by the Deutsche Akademische Austauschdienst.

References

[1] F.A. Lewis, The Palladium–Hydrogen System, Academic Press, New York, 1967.
[2] S. Niwa, M. Eswaramoorthy, J. Nair, A. Raj, N. Itoh, H. Shoji, T. Namba, F. Mizukami, Science 295 (2002) 105.
[3] G.L. Holleck, J. Phys. Chem. 74 (1970) 503.
[4] J. Shu, B.P.A. Grandjean, A. van Neste, S. Kaliaguine, Can. J. Chem. Eng. 69 (19911036).
[5] E. Wicke, G.H. Nernst, Ber. Bunsenges. Phys. Chem. 68 (1964) 224.
[6] T.L. Ward, T. Dao, J. Membr. Sci. 153 (1999) 211.
[7] B.A. McCool, Y.S. Lin, J. Mater. Sci. 36 (2001) 3221.
[8] Arguably, the distinction between a hydrogen solution and a hydride is somewhat arbitrary since the latter can be considered a concentrated hydrogen solution as well. But for the sake of simplicity, we refer to the dilute hydrogen solution phase in the following when we use the terms solution and solubility, because hydrogen solubilities have been in general determined in the limit of infinite dilution.
[9] M. Hansen, Constitution of Binary Alloys, McGraw-Hill, New York, 1958.
[10] S. Wieland, T. Melin, A. Lamm, Chem. Eng. Sci. 57 (2002) 1571.
[11] J. Völkl, G. Alefeld, Diffusion of hydrogen in metals, in: G. Alefeld, J. Völkl (Eds.), Hydrogen in Metals I, vol. 28, Springer-Verlag, Berlin, 1978, p. 321.
[12] R. Burch, R. Buss, J. Chem. Soc. I, Faraday Trans. 71 (1975) 913.
[13] D. Fisher, D.M. Chisdes, T.B. Flanagan, J. Solid State Chem. 20 (1977) 149.
[14] T.B. Flangan, S. Luo, D. Clewley, J. Alloy Compd. 356–357 (2003) 13.
[15] S. Uemiya, N. Sato, H. Ando, Y. Kude, T. Matsuda, E. Kikuchi, J. Membr. Sci. 56 (1991) 303.
[16] F. Roa, J.D. Way, R.L. McCormick, S.N. Paglieri, Chem. Eng. J. 93 (2003) 11.
[17] X.L. Pan, G.X. Xiong, S.S. Sheng, N. Stroh, H. Brunner, Commun. Chem. (2001) 2536.
[18] X.L. Pan, N. Stroh, H. Brunner, G.X. Xiong, S.S. Sheng, J. Membr. Sci. 226 (2003) 111.
[19] X.L. Pan, N. Stroh, H. Brunner, G.X. Xiong, S.S. Sheng, Sep. Purif. Technol. 32 (2003) 265.
[20] Before this set of experiments started, the membrane already had been operated in hydrogen atmosphere for 3 months between 200–500 °C.
[21] Y. Sakamoto, N. Ishimaru, Y. Mukai, Ber. Bunsenges. Phys. Chem. 95 (1991) 680.
[22] R.C. Hurlbert, J.O. Konencny, J. Chem. Phys. 34 (1961) 655.
[23] D.W. Breck, Zeolite Molecular Sieves, Wiley, New York, 1973.
[24] B.D. Morreale, M.V. Ciocco, R.M. Enick, B.I. Morsi, B.H. Howard, A.V. Cugini, K.S. Rothenberger, J. Membr. Sci. 212 (2003) 87.
[25] O.J. Kleppa, P.C. Shamsuddin, J. Chem. Phys. 71 (1979) 1656.
[26] A.S. Zetkin, G.E. Kagan, A.N. Varaskin, E.S. Levin, Sov. Phys. Solid State 34 (1992) 83.
[27] B. Huber, G. Sicking, Phys. Stat. Sol. A 47 (1978) 85.
[28] P. Kamakoti, D.S. Sholl, J. Membr. Sci. 225 (2003) 145.
[29] R. Taylor, J. Inst. Met. 54 (1934) 255.
[30] F.W. Jones, C. Sykes, J. Inst. Met. 65 (1939) 419.
[31] J. Piper, J. Appl. Phys. 37 (1966) 715.
[32] V.F. Degtyareva, V.E. Antonov, I.T. Belash, E.G. Ponyatovskii, Phys. Stat. Sol. A 66 (1981) 77.